

Front Pinning and Localized States Analogues in Long-Delayed Bistable Systems

Francesco Marino,¹ Giovanni Giacomelli,² and Stephane Barland³

¹*CNR–Istituto Nazionale di Ottica, largo E. Fermi 6, I-50125 Firenze, Italy*

²*CNR–Istituto dei Sistemi Complessi, via Madonna del Piano 10, I-50019 Sesto Fiorentino, Italy*

³*Université de Nice Sophia Antipolis, Institut Non Lineaire de Nice, CNRS UMR 7335, 06560 Valbonne, France*

(Received 10 October 2013; published 10 March 2014)

Localized structures have been observed in many spatially extended systems of either biological, chemical, or physical nature. Here, we study experimentally front pinning and dissipative localized structures in a delayed optical system based on a bistable semiconductor laser with optoelectronic feedback. We observe that many of the concepts known to apply to spatially localized structures also apply in this context, with specificities related to the lack of reversibility symmetry. Numerical simulations based on purely prototypical modeling reproduce very well the experimental findings, which indicates that the results do not depend on the specific physical system under consideration, but are, on the contrary, very generic features of time delayed systems.

DOI: 10.1103/PhysRevLett.112.103901

PACS numbers: 42.65.Sf, 02.30.Ks, 05.45.-a

Nonlinear systems driven far from equilibrium often admit multiple coexisting stable attractors, and fronts connecting these states are fundamental in the formation of spatial structures. Therefore, a considerable amount of research has been devoted to the dynamics of fronts and how their interaction can lead to the stability of spatial localized structures. In large classes of systems, this stability relies on front “pinning”: even when two states have a different free energy, a front connecting them may be stationary provided one of the states is spatially modulated [1]. The presence of the spatial modulation, then, leads to an unfolding of the Maxwell point [2] into a “pinning region,” which is of fundamental importance since it contains the series of homoclinic bifurcations leading to the formation of families of localized states in spatially extended systems [3,4]. Localized states have been explained on the basis of this homoclinic snaking in many fields of science (see, e.g., [5,6]), in particular, in nonlinear optics (see, e.g., [7], several contributions in [8], and the review [9]). In the optical context, front pinning and unpinning have been recently studied close to a modulational instability in [10] and in a spatially forced optical system [11,12]. In the case of spatial forcing, the homoclinic snaking structure and localized states have been analyzed in [13,14].

Here, the analogue of pinning phenomena and spatially localized structures are demonstrated in a system with no spatial degrees of freedom.

A correspondence between delayed dynamical systems and one-dimensional spatially extended systems is expected in the long-delay limit, i.e., when the delay time τ is much higher than the typical time scale of the isolated system [15,16]. In this case, the space-time representation is obtained by mapping a delay-time segment onto a

pseudospacial cell and the index numbers of the subsequent delay cells, n , into a pseudotime variable.

While the formal equivalence has been rigorously demonstrated for systems undergoing a supercritical Hopf bifurcation [17,18], a proof in the case of subcritical bifurcations (i.e., to finite-amplitude solutions) is still lacking. Theoretical studies [19–24] and recent experiments [25,26] suggest that the representation could also be effective in these cases. In particular, finite amplitude solutions in long-delayed bistable systems translate into propagating fronts in the appropriate spatiotemporal framework [25]. However, whether the spatiotemporal analogy can be extended much further than the mere existence of propagating fronts is yet to be demonstrated.

In this Letter, we provide the experimental evidence of localized structures in a long-delayed bistable system. We show that a small-amplitude temporal modulation acts as a pseudospacial forcing, giving rise to front pinning phenomena and, thus, suggesting the analogy with a 1D spatially forced bistable medium. Moreover, due to the lack of reversibility symmetry in pseudospace, the unpinning transition occurs via two separated saddle-node bifurcations. The splitting of such a transition has, thus far, never been reported, even in the framework of spatially extended systems. Within the pinning range, we demonstrate the existence and stability of the analogue of single- and multicell spatially localized states. Such structures can be independently generated and erased by means of suitable external perturbations, thus, enabling their use as optical information bits. The results are well reproduced in the framework of a simple general model.

The experiment (top panel of Fig. 1) is based on a single transverse, vertical-cavity surface-emitting laser (VCSEL) in a regime of bistable emission for the two orthogonal, linear polarizations of the light intensity.

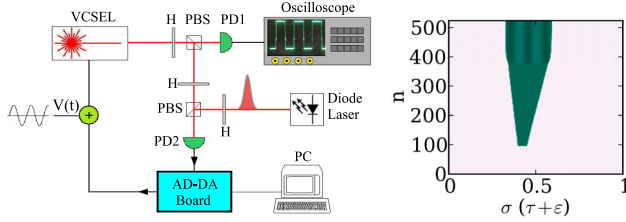


FIG. 1 (color online). Left panel: experimental apparatus. H: half-wave plates; PD: photodiodes; PBS: polarizing beam splitters; AD-DA: analog-to-digital, digital-to-analog converter. Right panel: space-time representation of the laser intensity signal, from light (lower level state) to dark (higher level state). A dark region of 0.05 space units (1 ms) is seeded at time $n = 100$. At $n = 387$, the modulation is switched on. Parameters: $\tau = 19$ ms, $G = 1$, $V_0 = -454$ mV, $V_m = 1$ mV, $T_m = 1.904$ ms, $\epsilon = 0.002\tau$.

The polarization components of the output beam are selected and split by means of a half-wave plate and a polarizing beam splitter. One polarization is sent to a high sensitivity detector whose output is monitored by a digital oscilloscope. The signal from the orthogonally polarized beam is sampled, sequentially shifted by means of a reconfigurable acquisition board, and then fed back into the laser through the pump current. In this way, a suitable control of the delay transfer function can be achieved, including the setting of initial conditions, the delay time τ (fixed here at 19 ms, much longer than any time scale of the system) and the coupling factor G (amplification of the feedback signal current). The laser, housed in a temperature-stabilized box, is biased by a voltage signal $V(t) = V_0$ to which a periodic modulation $V_m \sin(2\pi t/T_m)$ provided by a function generator can be superimposed. The amplitude of the modulation is always kept much smaller than the width of the bistability region. The operation point within the bistable region can be controlled either through the dc pump V_0 or through the coupling G , as shown in [25]. Here, we fix $V_0 = -454$ mV and we use G as the main control parameter. Pulse perturbations to the feedback loop can be applied by injecting light from a diode laser driven by a pulsed current. The space-time representation is obtained by decomposing the time series into pseudospacial cells of length $\tau + \epsilon$. Each time value within the time trace is identified by a real number σ ($0 \leq \sigma < \tau + \epsilon$), indicating the “position” inside a given delay segment and, thus, acting as a pseudospacial variable, and by the segment number n , which plays the role of the pseudotime coordinate. The parameter $\epsilon \ll \tau$ has been chosen so that the temporal modulation $V_m \sin(2\pi t/T_m)$ translates into a stationary periodic pattern along the σ axis.

In the absence of periodic forcing ($V_m = 0$) and for the chosen value of V_0 , the system exhibits bistability between a low-intensity and a high-intensity state. When the system is prepared in an inhomogeneous state, in which the whole feedback loop is filled with the low power state with the exception of a small segment in the high-power state, the

system displays coarsening; i.e., fronts start to propagate such that a single phase (the dominant) progressively invades the whole system [25]. An example is shown in the right panel of Fig. 1, where left and right fronts connecting the low to high power states (and back) drift apart, leading to a growth of the high intensity domain. At time $n = 378$, the (pseudo)spatial modulation is applied. Starting from that instant, the motion of the fronts is altered by the modulation and, after a short transient, is blocked. Notice that the coarsening pattern in Fig. 1 is slightly asymmetric. This is due to the fact that, at each subsequent delay interval, the average position of a phase domain shifts to the right by a quantity δ , which depends on the system parameters [25]. This is a general property of long-delayed systems [17,18,27]. A symmetric coarsening pattern together with a stationary pseudospacial modulation could, thus, be obtained by choosing $\epsilon = \delta$ in the space-time representation and by setting T_m as an integer submultiple of $(\tau + \delta)$.

At this point, we have a basic demonstration of the freezing of coarsening caused by the pinning of fronts via a pseudospacial modulation. In systems with spatial forcing, the transition from the pinning to the propagation regime occurs via a saddle node (on a circle-) bifurcation for the velocity of the fronts [28]. This translates into an average growth rate of the area occupied by the most stable state, which scales as the square root of the distance to the unpinning point [12].

In order to study this transition, we perform systematic measurements for different values of the parameter G which controls the asymmetry of states. For each value of G , the system is prepared in an initial condition consisting of the whole space in the low power state with the exception of a segment in the high power state. The results are shown in Fig. 2.

For small values of the asymmetry parameter, the fronts do not propagate at all and, accordingly, the growth rate is zero. We remind that, in absence of forcing (as in spatially

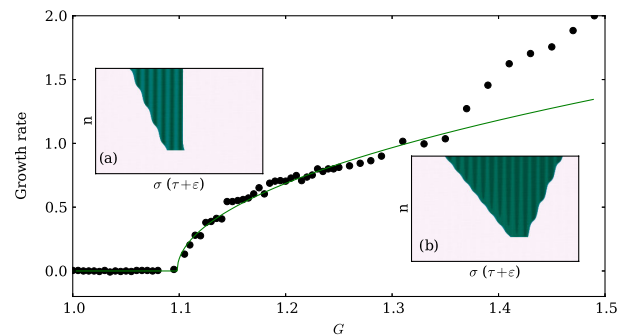


FIG. 2 (color online). Growth rate of the dominant phase against the coupling parameter G . Solid line: square-root fit in the range $1 \leq G \leq 1.3$. Insets: Space-time representation of the laser intensity for $G = 1.2$ [(a)] and $G = 1.47$ [(b)]. Other parameters as in Fig. 1.

extended bistable systems), this happens only at the Maxwell point as shown in Ref. [25]. The observation of a zero growth rate in a finite region, therefore, corresponds to the unfolding of the Maxwell point. Above $G = 1.1$, the growth rate suddenly increases with a square-root scaling, indicating that the unpinning transition has occurred. However, only the left front is propagating, whereas the right front is still pinned [see inset (a) in Fig. 2]. The situation remains qualitatively unaltered until $G = 1.32$, where a second bifurcation takes place, as is clearly illustrated by the abrupt change in the growth rate. This corresponds to the unpinning of the right front [inset (b)]. The other front now also drifts away (as shown on the bottom right inset in Fig. 2), such that the high power state invades the whole system. Although a detailed study of this splitting and of each of the transitions is left for future work, the scaling of the growth rate and the oscillating front velocity visible at the edges of the domain suggest that the two subsequent bifurcations are saddle-node ones.

Within the pinning region, one expects to observe localized states, consisting of pairs of stationary fronts connecting back and forth the lower and upper states. In order to generate such structures, the system is prepared in the low power state, with G within the pinning region. At time $n = 100$, an additional laser pulse is applied to the feedback loop, locally switching the system to the higher state. Since the pulse is much shorter than a round-trip time, it plays the role of a local perturbation in the pseudospace. The results are shown in Fig. 3 where, after a transient, a localized structure is generated and remains unaltered until the experiment is switched off. Since, by definition, localized states are expected to have only short range interactions, several of them can exist independently of each other provided they are separated enough in space. This is shown in the left panel's inset of Fig. 3, in which

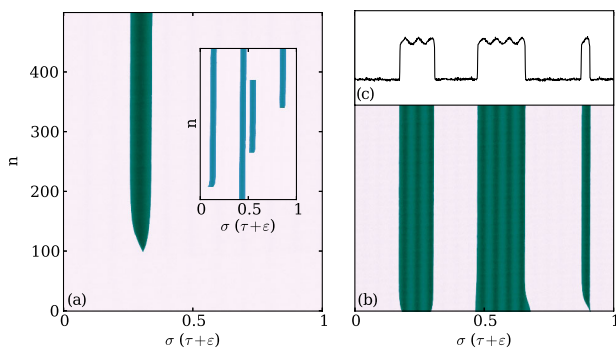


FIG. 3 (color online). (a) Generation of a single-cell localized structure from a rectangular initial condition. Inset: Generation and annihilation of independent structures by applying optical perturbations into the feedback loop. (b) Single- and multihump localized structures, and (c) the corresponding transverse profile at $n = 400$. The initial condition is a sum of three rectangular functions of widths $w_0 \approx 0.11\tau$, 0.21τ , $3.1 \times 10^{-3}\tau$. Other parameters as in Fig. 1.

several localized states have been nucleated and annihilated by short optical perturbations [29]. Although the existence of a homoclinic snaking phenomenon for localized structures analogues in delayed dynamical systems remains to be established, we have observed the coexistence of not only single-hump, but also multihump localized states. In the right panel of Fig. 3, the parameters are set within the pinning region, and we set as initial conditions three islands (of differing widths) of high power state on a lower state background. During the following transient, each of the seeded areas evolves towards a different state, corresponding to three-, four-, and single-hump localized states. This result demonstrates that such structures can coexist in the system, in direct analogy to what was observed in spatially modulated bistable systems [14].

The polarization dynamics of vertical-cavity surface-emitting lasers can be described by means of a one-dimensional bistable potential [30,31]. Here, for the sake of simplicity and generality, we adopt a completely prototypical model of a bistable system with delayed feedback [25].

$$\dot{x} = -U'(x) + gx(t - \tau), \quad (1)$$

where the scalar variable $x(t)$ represents the laser intensity, $g > 0$ is the feedback gain [32], and $U'(x) = x(x + 1 + a)(x - 1)$. Along with the trivial unstable solution $x_0 = 0$, Eq. (1) possesses two stable fixed points $x_{\pm} = [-a \pm \sqrt{(2+a)^2 + 4g}]/2$. The parameter a controls the degree of stability of the two stable states or, equivalently, the asymmetry of the double-well potential, $U(x)$.

As in the experiment, we apply a small temporal modulation to the asymmetry parameter a , i.e., $a = a_0 + a_m \sin(2\pi t/T)$ and we integrate numerically Eq. (1). We choose the modulation period close to an integer submultiple of $(\tau + \delta)$, and we use $\varepsilon = \delta$ in the space-time representation. In this case, the pattern is stationary in the pseudotime.

In absence of modulation, the growth rate of the dominant phase (dashed line in Fig. 4) increases with $|a_0|$ and is zero only at the Maxwell point, $a_0 = 0$. When $a_m > 0$, the homogeneous states x_{\pm} become periodic states in the pseudospace. In spatial systems, the fronts remain pinned even for finite values of a_0 , while propagating with a velocity oscillating around a nonzero mean value for larger asymmetry parameters. In Fig. 4, we plot the average fronts velocity as a function of a_0 , for two values of the modulation amplitude (solid curves). For parameters next to the Maxwell point, we observe the existence of a pinning region where the fronts velocity is zero. Outside this range, a regime is found where one of the fronts starts propagating while the other remains motionless [see inset (a)]. For larger values $|a_0|$, also, the second front is eventually unpinned [inset (b)]. Both transitions occur via saddle-node bifurcations in the front velocity. The results are in

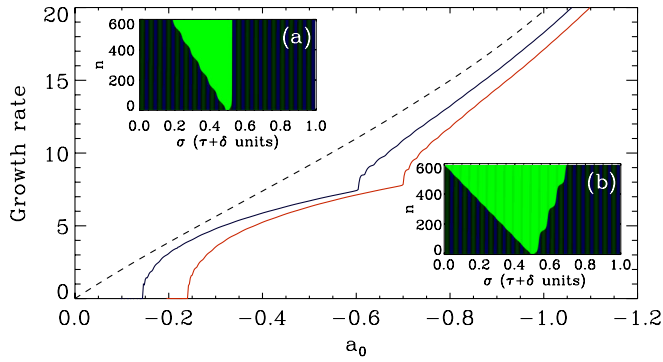


FIG. 4 (color online). Average growth rate of the dominant phase against a_0 for $a_m = 0$ (dashed curve), $a_m = 0.3$ blue (dark) solid curve and $a_m = 0.4$ red (light) solid curve. Insets: Spatiotemporal plots corresponding to $a_m = 0.4$ and $a_0 = -0.4$ [inset (a)] and $a_0 = -0.8$ [inset (b)]. The initial condition is a rectangular-function profile $x_0(t)$ with $w_0 = 0.02\tau$ (see text). Other parameters: $g = 1$, $\tau = 100$, $T = (\tau + \delta)/20$, $\delta \approx 1.3 \cdot 10^{-3}\tau$.

excellent qualitative agreement with the experimental observations reported in Fig. 2. This behavior is reminiscent of what is observed in 1D spatially periodic media, where the presence of a spatial periodicity is known to induce an energy barrier for the front propagation to occur. Here, however, the transition from the pinning to the propagation regime occurs via two separated saddle-node bifurcations. When we increase the modulation amplitude, the pinning region grows, whereas the average front speed decreases.

Within the pinning region, stationary stable localized states can be generated in two different ways: by preparing the system in a suitable initial condition, or in response to an external perturbation. An example is shown in Fig. 5(a), demonstrating the coexistence of multihump solutions for the considered parameters. In order to verify the mutual independence of localized structures, we start from a homogeneous initial condition $x_0(t) = x_-$ and we add to Eq. (1) a sequence of rectangular pulses $P(t) = p_0 \text{rect}[(t - t_i)/w_i]$. In response to each perturbation, the system undergoes a transient regime until a stable stationary localized state is generated [Fig. 5(b)]. As expected, each structure remains totally unperturbed by the creation of other nearby structures at subsequent times. Since the spatial width of the addressing pulses is much narrower than that of the modulation period, here, we generate only single-hump localized states. Localized states can also be individually erased by means of a suitable local perturbation. To this end, we apply a pulse with negative amplitude at the spatial position where a localized state was previously created. In response to the perturbation, the structure is switched off, leaving the other structures unaffected. The phenomenology here described perfectly matches the experimental findings shown in Fig. 3.

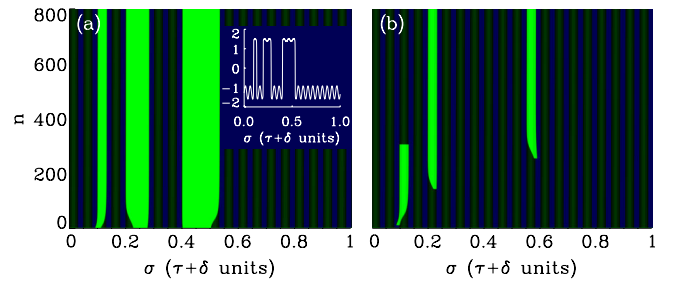


FIG. 5 (color online). (a) Single- and multihump localized structures and the corresponding transverse profile at $n = 700$ (inset). The initial condition is a sum of three rectangular functions centered at 0.1τ , 0.25τ , 0.45τ , and widths $w_0 = 0.02\tau$, 0.05τ , 0.1τ . (b) Nucleation and erasing of single-hump localized structures. Addressing pulses $P(t)$ with $w_t = 2$ and $p_0 = 1$ (see text) of $w_\sigma \approx 0.02$ are applied at $(\sigma_1, n_1) \approx (0.09, 10)$, $(\sigma_2, n_2) \approx (0.22, 140)$, $(\sigma_3, n_3) \approx (0.58, 250)$. The erasing pulse ($w_t = 4$, $p_0 = -1$) is applied at $(\sigma_4, n_4) \approx (0.09, 300)$. Modulation parameters: $a_0 = -0.2$ and $a_m = -0.4$. Other parameters as in Fig. 4.

In conclusion, we have shown the occurrence of front pinning phenomena and localized states in a long-delayed, bistable system. Our results demonstrate that many concepts associated to spatially localized structures also apply in this framework. In addition, due to the absence of the reversibility symmetry in the pseudospace, the splitting of the unpinning transition is reported. While extending the validity of the space-time analogy and verifying several features of front dynamics, we expect our results to possibly trigger new directions of theoretical and experimental research. Moreover, the possibility of independently generating and erasing localized states might enable their use as bits in faster, suitably designed, all-optical setups.

S. B. acknowledges funding from Agence Nationale de la Recherche through Grant No. ANR-12-JS04-0002-01.

-
- [1] Y. Pomeau and P. Manneville, *Commun. Math. Phys.* **74**, 189 (1980).
 - [2] P. Coullet, *Int. J. Bifurcation Chaos Appl. Sci. Eng.* **12**, 2445 (2002).
 - [3] P. Coullet, C. Riera, and C. Tresser, *Phys. Rev. Lett.* **84**, 3069 (2000).
 - [4] J. Burke and E. Knobloch, *Chaos* **17**, 037102 (2007).
 - [5] E. Meron, *Ecol. Model.* **234**, 70 (2012).
 - [6] M. Tlidi, M. Taki, and T. Kolokolnikov, *Chaos* **17**, 037101 (2007).
 - [7] S. Barbay, X. Hachair, T. Elsass, I. Sagnes, and R. Kuszelewicz, *Phys. Rev. Lett.* **101**, 253902 (2008).
 - [8] R. Kuszelewicz, S. Barbay, G. Tissoni, and G. Almuneau, *The Eur. Phys. J. D* **59**, 1 (2010).
 - [9] T. Ackemann, W. J. Firth, and G.-L. Oppo, in *Advances in Atomic Molecular and Optical Physics*, edited by P. R. B. E. Arimondo and C. C. Lin (Academic Press, New York, 2009), Vol. 57, pp. 323–421.

- [10] M. Pesch, W. Lange, D. Gomila, T. Ackemann, W. J. Firth, and G. L. Oppo, *Phys. Rev. Lett.* **99**, 153902 (2007).
- [11] F. Haudin, R. G. Elías, R. G. Rojas, U. Bortolozzo, M. G. Clerc, and S. Residori, *Phys. Rev. Lett.* **103**, 128003 (2009).
- [12] F. Haudin, R. G. Elías, R. G. Rojas, U. Bortolozzo, M. G. Clerc, and S. Residori, *Phys. Rev. E* **81**, 056203 (2010).
- [13] D. Gomila and G.-L. Oppo, *Phys. Rev. A* **76**, 043823 (2007).
- [14] F. Haudin, R. G. Rojas, U. Bortolozzo, S. Residori, and M. G. Clerc, *Phys. Rev. Lett.* **107**, 264101 (2011).
- [15] F. T. Arecchi, G. Giacomelli, A. Lapucci, and R. Meucci, *Phys. Rev. A* **45**, R4225 (1992).
- [16] M. Wolfrum and S. Yanchuk, *Phys. Rev. Lett.* **96**, 220201 (2006).
- [17] G. Giacomelli and A. Politi, *Phys. Rev. Lett.* **76**, 2686 (1996).
- [18] G. Giacomelli and A. Politi, *Physica (Amsterdam)* **117D**, 26 (1998).
- [19] E. V. Grigorieva, S. A. Kashchenko, N. A. Loiko, and A. M. Samson, *Physica (Amsterdam)* **59D**, 297 (1992).
- [20] S. N. Chow, J. K. Hale, and W. Huang, *Proc. R. Soc. Edinburgh, Sect. A: Math.* **120**, 223 (1992).
- [21] M. Nizette, *Physica (Amsterdam)* **183D**, 220 (2003).
- [22] M. Nizette, *Phys. Rev. E* **70**, 056204 (2004).
- [23] M. Nizette, D. Rachinskii, A. Vladimirov, and M. Wolfrum, *Physica (Amsterdam)* **218D**, 95 (2006).
- [24] D. W. Sukow, A. Gavrielides, T. Erneux, B. Mooneyham, K. Lee, J. McKay, and J. Davis, *Phys. Rev. E* **81**, 025206 (2010).
- [25] G. Giacomelli, F. Marino, M. A. Zaks, and S. Yanchuk, *Europhys. Lett.* **99**, 58005 (2012).
- [26] L. Larger, B. Penkovsky, and Y. Maistrenko, *Phys. Rev. Lett.* **111**, 054103 (2013).
- [27] G. Giacomelli, R. Hegger, A. Politi, and M. Vassalli, *Phys. Rev. Lett.* **85**, 3616 (2000).
- [28] R. Rojas, Ph. D. thesis, Université de Nice Sophia-Antipolis, 2005.
- [29] A localized state is nucleated by shining a light pulse into the feedback loop, and it can, subsequently, be digitally squashed.
- [30] M. P. Van Exter, M. B. Willemsen, and J. P. Woerdman, *Phys. Rev. A* **58**, 4191 (1998).
- [31] G. Giacomelli and F. Marin, *Quantum Semiclass. Opt.* **10**, 469 (1998).
- [32] The numerical parameter g is not trivially related to the experimental parameter G , as analyzed in [25].